J Mater Sci (2011) 46:6783–6793
DOI 10.1007/s10853-011-5636-z

Microstructure evolution and elemental diffusion of SiCp/Al–Cu–Mg composites prepared from elemental powder during hot pressing

Q. Zhang · B. L. Xiao · Z. Y. Liu · Z. Y. Ma

Received: 29 March 2011 / Accepted: 13 May 2011 / Published online: 1 June 2011

Abstract 15vol%SiCp/Al–Cu–Mg composites were fabricated by hot pressing method using pure elemental powders. Microstructure evolution and elemental diffusion of Cu and Mg were studied. The microstructure of as-hot pressed composites and the elemental distribution of the composites before and after solution treatment were also investigated. The results showed that there were two types of eutectic liquid phases with different compositions after the compact was heated to 580 °C. After the compact was held at 580 °C for 60 min, the eutectic liquid was absorbed into the Al matrix and some equilibrium liquid phases formed in the boundaries of the initial Al particles. Meanwhile, Cu was homogeneously distributed in the Al particles while Mg tended to be distributed near the boundaries of the initial Al particles and in the SiC clusters. The presence of Al_2Cu, Mg_2Si, and some oxides of Mg was identified in the as-hot pressed composite. After solution treatment, Al_2Cu dissolved into the Al matrix, however, some Mg-rich compounds (silicide and oxide of Mg) did not dissolve into the matrix completely.

Introduction

Particle-reinforced aluminum matrix composite (PRAMC) is a class of advanced materials providing ideal properties such as high specific strength, high specific modulus, low coefficient of thermal expansion, and good wear resistance [1, 2]. A wide range of production techniques have been developed for PRAMCs fabrication, including stir casting, pressure infiltration, spray deposition, and powder metallurgy (PM) [3]. Among these methods, PM is generally preferred since it offers a number of advantages [3]. Most importantly, execution of the PM process under the solid state minimizes the deleterious reactions between the metal matrix and the ceramic reinforcement, resulting in the improved mechanical properties of the PRAMCs, especially ductility compared with other methods [4, 5].

Over the last two decades, fabricating parameters, microstructure and mechanical properties of PRAMCs with a variety of matrix alloys (such as 2xxx series, 6xxx series, and 7xxx series) through the PM method were extensively studied [6–8]. The composites in these studies were usually fabricated using pre-alloyed aluminum powder prepared by inert-gas atomization. However, it is costly and time assuming for mass production [3]. By comparison, using pure elemental powders could not only reduce the cost and periods, but also provide an extra advantage of modifying the matrix alloy compositions easily.

The previous studies indicated that for fabricating PRAMCs using elemental powders through the PM technique, the formation of liquid phase and the diffusion of alloying elements into Al particles during sintering or hot pressing (HP) were the key issues [9–11]. Kim et al. [9] investigated the sintering process of SiCp/Al–7.3 wt%Cu composite using pure Al and Cu powders. It was showed that copper addition was helpful for densification of the composite during sintering because some Cu-rich liquid phases were formed to fill most of the powder boundaries and voids associated with SiC particles. Zhou et al. [10] studied the sintering process of 10%SiCp/2014 (Al–4.5Cu–0.5 Mg) composite. They found that Al_2Cu (θ phase) was the main intermetallic phase in the as-sintered composite. After the compact was sintered for 30 min, large discrete

Q. Zhang · B. L. Xiao (✉) · Z. Y. Liu · Z. Y. Ma
Shenyang National Laboratory for Materials Science, Institute of Metal Research, Chinese Academy of Sciences, Shenyang 110016, China
e-mail: blxiao@imr.ac.cn

Al_2Cu phase particles were found at the grain boundaries, and after 60 min of sintering, most of the Al_2Cu phase particles were dissolved into Al particles. However, the effect of Mg addition on the sintering behavior was not investigated in their article. Ogel et al. [11] studied the process of the liquid phase formation in Al–5Cu compacts during HP by quenching experiments. It was revealed that the eutectic liquid phase formed near the original sites of Cu particles at 550 °C, and formed a continuous network along the Al powder surfaces at 600 °C.

As far as we know, the previous studies about sintering or HP process of elemental powders were mostly focused on the Al–Cu binary matrix. For the most widely used SiCp/Al–Cu–Mg composites, few related studies were reported [10]. In this article, we chose pure Al, Cu, Mg, and SiC powders as raw materials and studied the process of liquid phase formation and the elemental diffusion of the SiCp/Al–Cu–Mg composites during HP. For this purpose, quenching experiments were carried out to freeze the microstructure at different stages of HP. The aim of this study is to understand alloying and densification processes of elemental powders. This will be beneficial to establish the HP procedure of PRAMCs based on elemental powders.

Experimental

Commercial pure Al powders (average size 13 μm, 99.9 pct purity, Angang Group Aluminium Powder Co., Ltd.), pure Cu powders (average size 13 μm, 99.5 pct purity, Wuxi ShunDa Metal Powder Co., Ltd.), and pure Mg powders (average size 32 μm, 99.5 pct purity, Tang-Shan WeiHao Magnesium Powder Co., Ltd.) were used as raw materials. Figure 1 shows the morphologies of these powders. The Al and Mg particles were spherical shape while the Cu particles exhibited a flake appearance. A nominal composition of Al–4.5Cu–1.8 Mg (wt%) was adopted as the matrix alloy. The SiC (average size 3.5 μm, 99 pct purity, White Dove (Group) Co., Ltd.) addition was 15% by volume. Metal powders were blended with SiC powders in a bi-axis rotary mixer for 8 h. The mixed powders were cold compacted into billets with a height of 30 mm and a diameter of 55 mm in a steel die under a pressure of 20 MPa. Then the compacts were pressed at a pressure of 50 MPa in a vacuum chamber of 10^{-2} Pa after being held at 580 °C for 60 min. For comparison, the corresponding matrix alloy was also fabricated by the same method. Part of the billets with the die was water quenched during the HP process. The cooling time of the billets with the die from 580 °C to room temperature was measured to be about 15 s. The specifications of the samples in this study are shown in Table 1.

Differential scanning calorimetry (DSC TA-Q1000) was conducted on a small piece of sample (50 mg) cut from the cold compact in the flowing argon atmosphere with a heating rate of 5 °C/min. The microstructures of the composites were examined under scanning electron microscope (SEM, quanta 600) and transmission electron microscope (TEM, TECNAI20). Thin foil for TEM was prepared by the ion-milling technique. An X-ray diffraction analyzer (D/max 2400) was used to identify the phases of the composites. The compositions of the phases and the matrix of the composites were determined by energy-dispersive spectrometry (EDS). The elemental distribution in the composites was examined by electron probe micro analysis (EPMA-1610).

Results

Figure 2 shows the DSC curve of the cold compact. Four endothermic peaks and one exothermic peak are detected in Fig. 2. According to the previous studies [3, 7], the endothermic pecks located at 649 and 636 °C corresponded to the melting of Al, and the exothermic peak at 642 °C corresponded to the reaction between molten Al and SiC. Because this reaction took place during the melting of Al, the melting peak of Al was divided into two peaks. Below the HP temperature in this study (580 °C), two endothermic peaks were detected. One was located at around 446 °C, and the other was located at around 525 °C, which indicated that some exothermic reactions take place before 580 °C.

Figure 3 shows the microstructures of samples 1 through 4. For samples 1 and 2, the boundaries of the initial Al particles were clear, and there existed many voids in the Al powder boundaries and the SiC clusters. Furthermore, some big voids with sizes of about 20–30 μm were found. With the increase of the holding time at 580 °C (samples 3 and 4), most of the voids in the Al powder boundaries disappeared and some sintering-necking formed between two contacted Al particles. Some voids were still found in the SiC clusters in samples 3 and 4. A few of intermetallic particles (white particles in Fig. 3) were found in samples 1–4. EDS analyses indicated that these intermetallic particles had two types of compositions, one contained Al, Cu, and Mg, the other contained Al and Cu. For convenience in this manuscript, we denoted the intermetallics containing Al, Cu, and Mg as phase A, and the intermetallics containing Al and Cu as phase B.

In sample 1, the white phases exhibited irregular shape and had a size of about 5–20 μm. Both phases A and B were identified. Phase A was usually located near the big voids and the atom percents of Al, Cu, and Mg were 69.7, 18.0, and 12.3%, respectively (Table 2). Phase B was usually located at the boundaries of the original Al

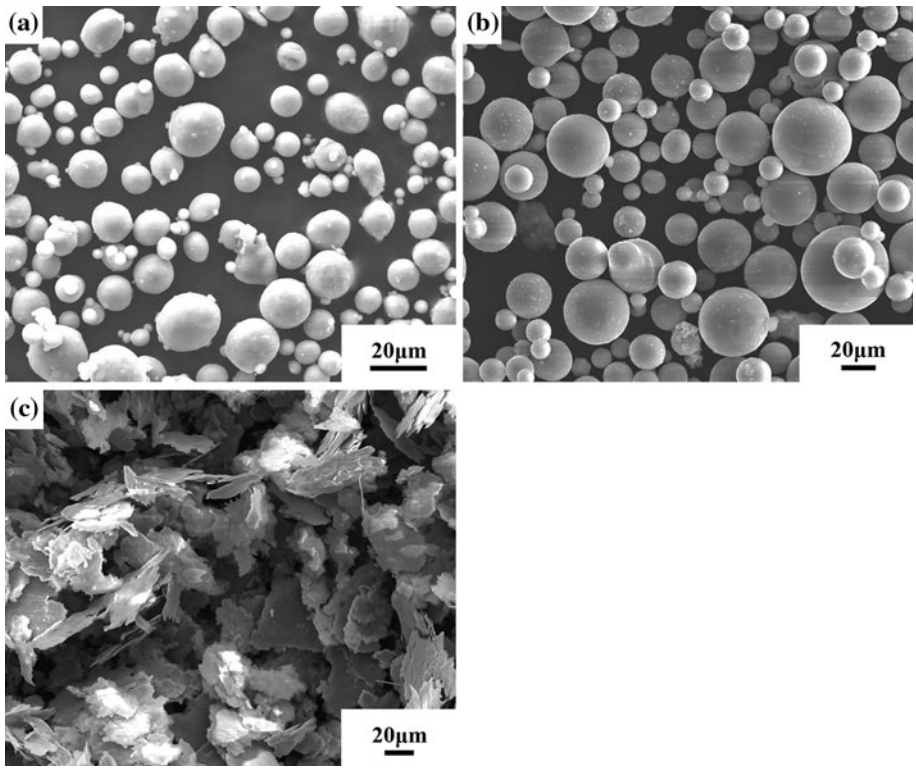

Fig. 1 SEM micrographs showing morphologies of as-received powders: **a** Al, **b** Mg, and **c** Cu

Table 1 The specifications of the samples in this study

Sample no.	Heating time (min)	Holding time in 580 °C (min)	HP or not	Cooling method after HP
1	180	0	No	Quenching
2	180	15	No	Quenching
3	180	30	No	Quenching
4	180	60	No	Quenching
5	180	60	Yes	Quenching
6	180	60	Yes	Furnace cooling
7[a]	180	60	Yes	Furnace cooling

[a] Matrix alloy

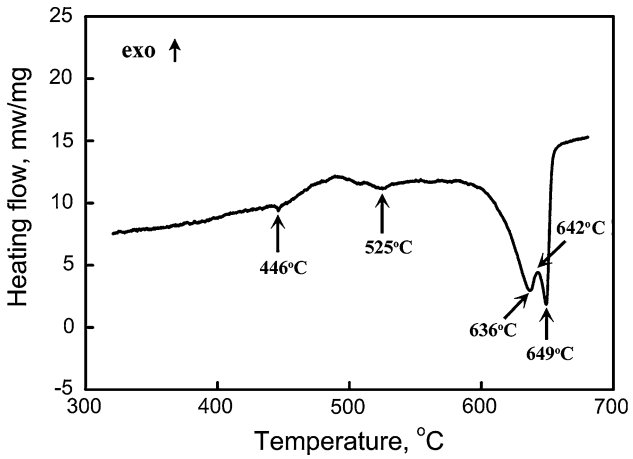

Fig. 2 The DSC curve of the cold compact

powders, and the atom percents of Al and Cu were 55.3 and 44.7%, respectively (Table 2). In addition, the variance of the compositions of phase B was rather large compared with that of phase A, which indicated that the compositions of phase B fluctuated greatly in different locations. In sample 2, the type and the morphologies of the white phases were similar to that in sample 1, but the composition of the white phase particles changed. The concentration of Cu in phase B dropped to 28.8% compared with that in sample 1 (Table 2), while the variance of the composition of these phases became small. In sample 3, the number of the white phase particles decreased compared with that in samples 1 and 2 and their size reduced to about 2–3 μm (Fig. 3c). EDS analyses indicated that all the white phases in sample 3 were phase B and the composition was similar to that in sample 2 (Table 2). After the holding time at

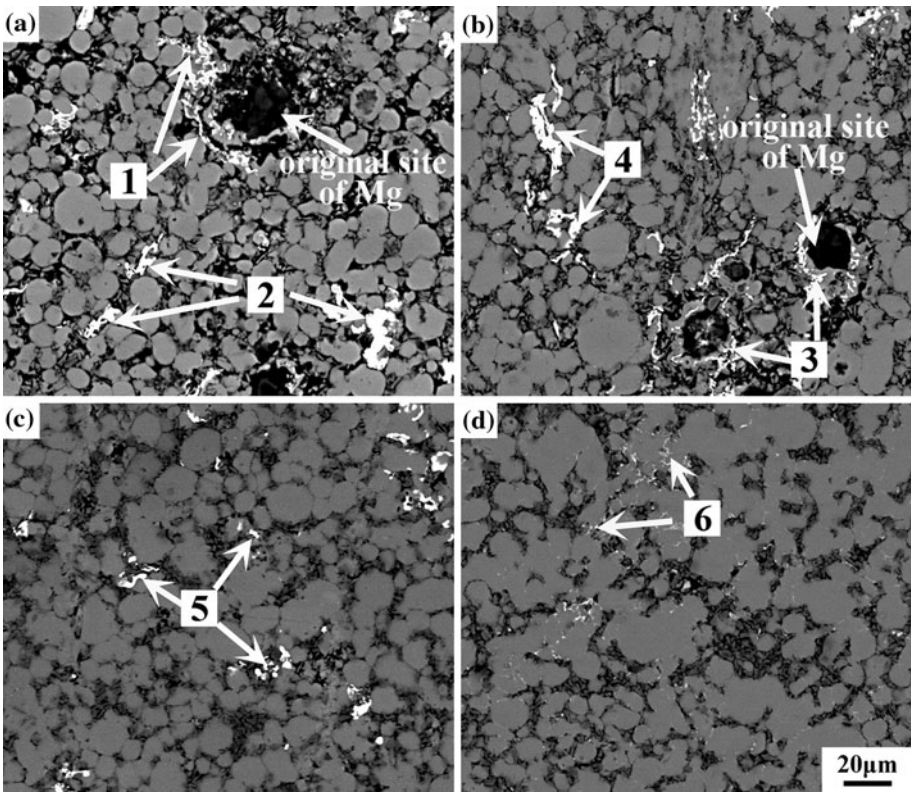

Fig. 3 SEM micrographs of **a** sample 1, **b** sample 2, **c** sample 3, and **d** sample 4

Table 2 Compositions of white phases in Fig. 3 (at%)

Analyzed phases	Al	Cu	Mg
1	69.7 ± 2.9	18.0 ± 1.9	12.3 ± 3.1
2	55.3 ± 16.2	44.7 ± 20.9	–
3	71.8 ± 3.8	17.0 ± 2.9	11.2 ± 3.6
4	67.6 ± 2.63	32.4 ± 3.7	–
5	71.2 ± 2.2	28.8 ± 4.0	–
6[a]	76.6 ± 1.6	14.1 ± 1.5	9.3 ± 1.7

All the values are obtained from at least ten analysis points

[a] The composition of phase 6 is approximate due to small size of the particles

580 °C extended to 60 min (sample 4), the white phases became very fine (<1 μm) and were distributed at the boundaries of the initial Al particles (Fig. 3d). EDS analyses show that the white phases were phase A, but the compositions of these white phases could not be accurately determined by EDS because their size was comparable with the diameter of electron beam of EDS.

Figure 4 shows the variation of concentration of Cu and Mg in the Al particles with the holding time at 580 °C. Three observations can be made from Fig. 4. First, with the increase of holding time at 580 °C, the concentration of Cu in the Al particles increased. After holding at 580 °C for 60 min, the concentration of Cu reached 3.3 wt% which was close to the equilibrium solubility of Cu in Al at 580 °C (about 3.5%) [12]. Second, at the early stage, the difference of the Cu concentration in different points was rather large, which indicated that the distribution of Cu was not homogeneous. After holding at 580 °C for 60 min, Cu was distributed more uniformly in the Al particles. Third, the Mg concentration in the Al particles increased with increasing the holding time at 580 °C at initial 15 min. After that, the Mg concentration did not increase with the holding time. It was noted that the Mg concentration was only half of the Mg addition and was much lower than the equilibrium solubility of Mg in Al at 580 °C (about 5%) when the compact was held at 580 °C for 60 min.

Figure 5 shows the elemental maps of sample 4. After the compact was held at 580 °C for 60 min, some fine Cu-rich intermetallics were found to be distributed at the boundaries of the initial Al particles (Fig. 5b), which was consistent with the result of Fig. 3d. In the Al particles, Cu was distributed uniformly, whereas Mg tended to be distributed at the boundaries of the Al particles and in the SiC clusters (Fig. 5b, c). Furthermore, some Mg-rich

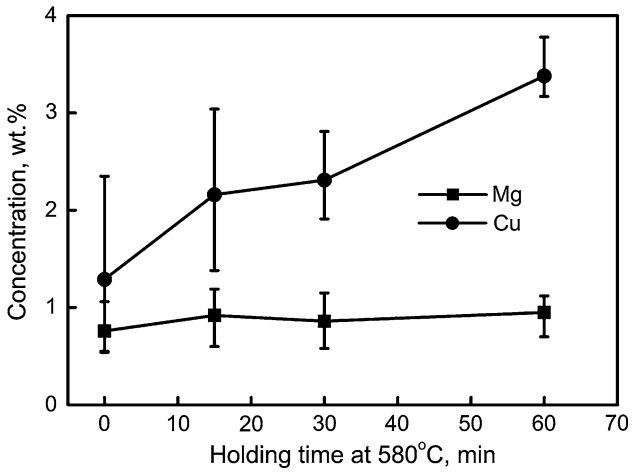

Fig. 4 Variation of concentration of Cu and Mg in Al particles with holding time at 580 °C

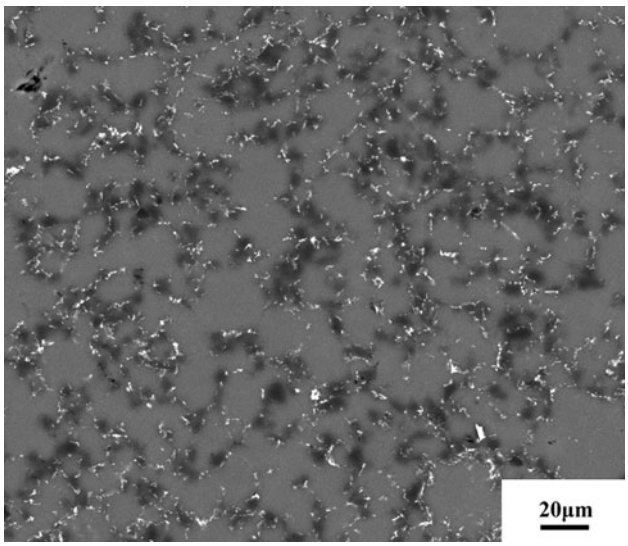

Fig. 6 SEM micrograph of sample 5

compounds were visible as shown in Fig. 5c, however, no evident aggregation of Cu was found at the locations corresponding to Mg-rich compounds (Fig. 5b, c).

Figure 6 shows the microstructure of sample 5. It can be seen that all the voids disappeared after HP. The number of the white phases in the matrix was more than that in sample 4 (Fig. 3d). The white phases were still distributed at the boundaries of the initial Al particles. Figure 7 shows the SEM micrograph and elemental maps of sample 6. As shown in Fig. 7, after the compact was slowly cooled to room temperature, the size of some Cu-rich intermetallics (marked by A in Fig. 7) was about 5 μm. EDS showed that the Cu-rich intermetallics had the composition of Al_2Cu.

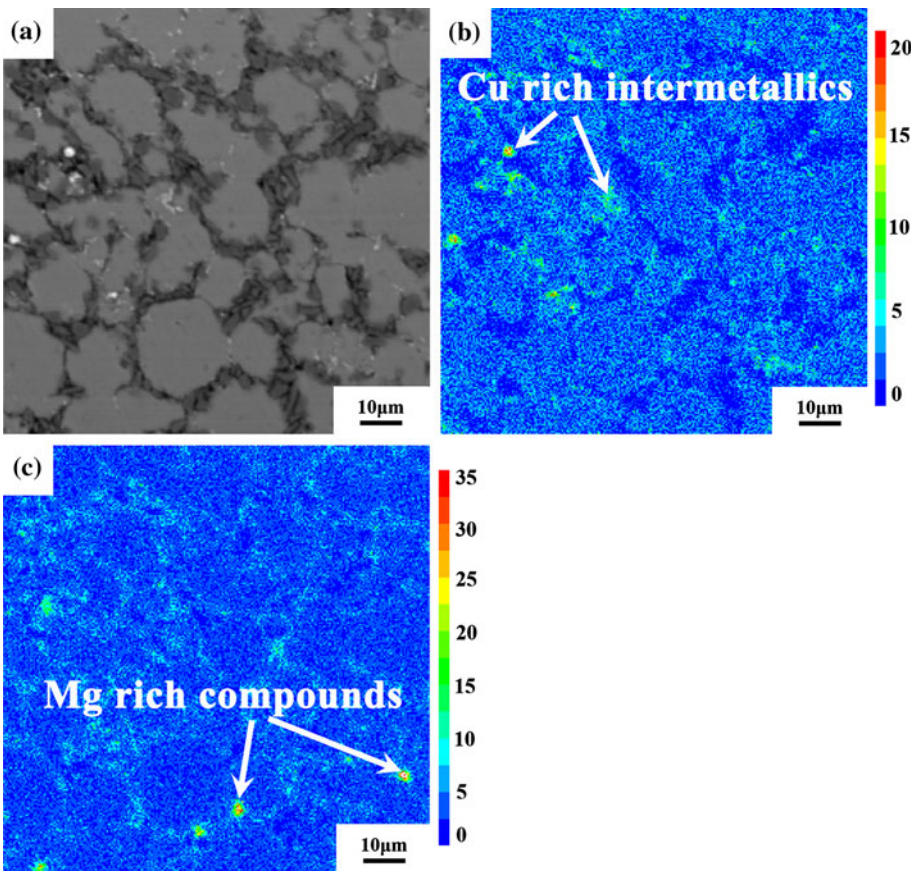

Fig. 5 Elemental maps of sample 4: **a** backscattered micrograph, **b** Cu map, and **c** Mg map

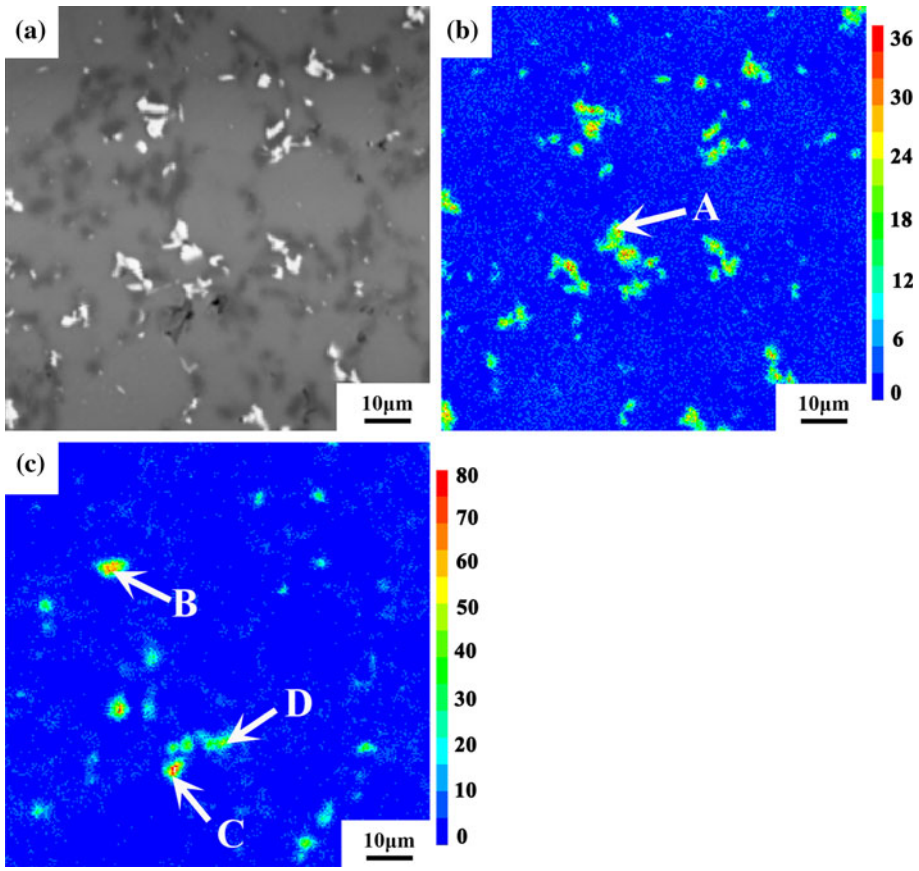

Fig. 7 Elemental maps of sample 6: **a** backscattered micrograph, **b** Cu map, and **c** Mg map

Table 3 The compositions of the phases in Figs. 8 and 10 (at%)

Analyzed point	Al	Cu	Mg	Si	O
A	67.7	32.3	–	–	–
B	26.2	–	32.6	–	41.2
C	16.1	–	47.5	4.6	31.8
D	9.2	–	53.9	36.9	–
E	11.0	–	58.2	30.8	–
F	2.6	–	40.9	6.2	50.3

In addition, some Mg-rich compounds (marked by B, C, and D in Fig. 7) were visible in sample 6. The EDS analyses indicated these phases were oxide and silicide of Mg (Table 3). TEM observation showed that some Mg_2Si blocks with the size of 1–2 μm formed near the SiC particles (Fig. 8).

Figure 9 shows the SEM micrograph and elemental maps of sample 6 after solution treatment. After the solution treatment, all the Cu-rich intermetallics dissolved into the matrix, and the Cu distribution become homogeneous in the matrix. However, there were still some Mg-rich compounds in sample 6 after the solution treatment (Fig. 9c). The compositions of these phases are shown in Table 3. They were determined to be oxide and silicide of Mg. Furthermore, Mg tended to be distributed at the boundaries of the initial Al particles and the clusters of SiC particles.

Figure 10 shows the XRD patterns of samples 6 and 7 before and after the solution treatment. For sample 7, the peaks of Al, Al_2Cu, and Al_2CuMg were detected in the XRD pattern, while for sample 6, the existence of SiC, Al, Al_2Cu, and Mg_2Si were identified. After the solution treatment, the peaks of intermetallics disappeared in the XRD pattern in both the samples 6 and 7.

Discussion

Formation of liquid phases during HP

Because the addition of Cu and Mg was only 4.5 and 1.8%, respectively, it is reasonable to assume that the Cu particles could not contact with the Mg particles in the cold

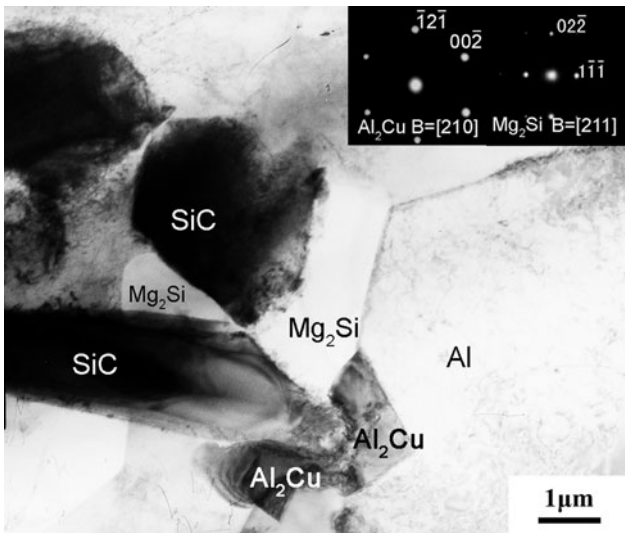

Fig. 8 TEM micrograph of sample 6

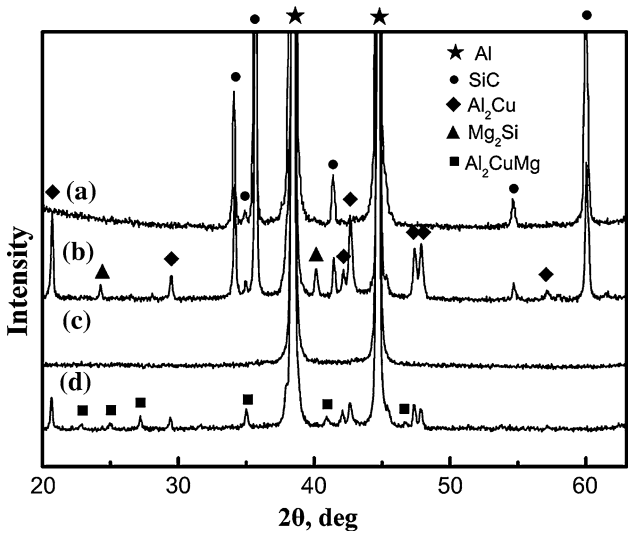

Fig. 10 XRD patterns of (*a*) sample 6 after solution treatment, (*b*) sample 6, (*c*) sample 7 after solution treatment, and (*d*) sample 7

compact. So at different zones of the cold compact, there existed only two different systems: the Al–Mg system and the Al–Cu system. The reference about the sintering behavior of Al–Mg is quite limited [13]. Based on the Al–Mg phase diagram [12], the product of reaction diffusion of the Al–Mg system is Mg_5Al_8 (β phase) when the mass fraction of Mg is less than 34% and the eutectic reaction takes place at 450 °C as follows:

$$\alpha(\mathrm{Al}) + \beta(\mathrm{Mg_5Al_8}) \Leftrightarrow \mathrm{L(liquid)(450\,^{\circ}C)}. \quad (1)$$

In this study, the DSC curve indicated that there was an endothermic peak at around 446 °C. It should correspond

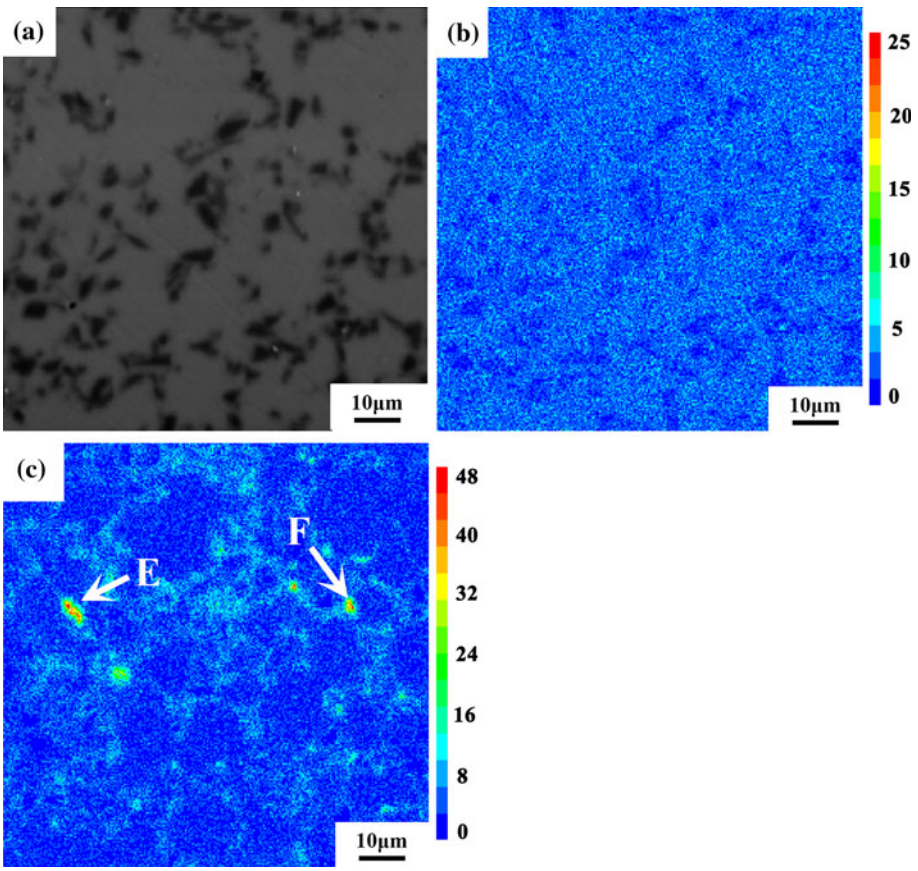

Fig. 9 Elemental maps of sample 6 after solution treatment: **a** backscattered micrograph, **b** Cu map, and **c** Mg map

to reaction 1. During the compact was heated from room temperature to 450 °C, some intermetallics such as Mg_5Al_8 would form because of solid diffusion near the original sites of the Mg particles. When the compact was heated to about 450 °C, reaction 1 took place (Fig. 2). The liquid phase from reaction 1 was Mg-rich liquid phase, thus Mg in the liquid phase would diffuse to Al through the liquid phase and left voids in the original sites of the Mg particles (Fig. 3a, b). If there were some Cu particles near the Mg-rich liquid phase, some ternary intermetallics such as Al_2CuMg (S phase) and Al_6CuMg_4 (T phase) would form, and eutectic reactions would take place in the following heating as follows [20]:

$$\alpha(\mathrm{Al}) + \mathrm{T}(\mathrm{Al_6CuMg_4}) \Leftrightarrow \mathrm{L}(\mathrm{liquid}) + \mathrm{S}(\mathrm{Al_2CuMg})(467\,^{\circ}\mathrm{C}) \quad (2)$$

$$\alpha(\mathrm{Al}) + \theta(\mathrm{Al_2Cu}) + \mathrm{S}(\mathrm{Al_2CuMg}) \Leftrightarrow \mathrm{L}(\mathrm{liquid})(507\,^{\circ}\mathrm{C}). \quad (3)$$

For the Al–Cu system, the previous studies about the sintering behavior of Al–7.3Cu [9] and Al–4.5Cu [10] suggested that Al_2Cu (θ phase) would form at the original sites of the Cu particles due to the solid diffusion between Al and Cu during heating. And the eutectic reaction between Al and Al_2Cu would take place at the Al/Al_2Cu interface when the temperature reached 548 °C:

$$\alpha(\mathrm{Al}) + \theta(\mathrm{Al_2Cu}) \Leftrightarrow \mathrm{L}(\mathrm{liquid})(548\,^{\circ}\mathrm{C}). \quad (4)$$

In this study, during the compact was heated to 580 °C, reactions 2, 3, and 4 might take place. The liquid phases formed by reactions 2 and 3 would contain Al, Cu, and Mg (phase A), and the liquid phase formed by reaction 4 would contain Al and Cu only (phase B). After quenching, the liquid phase would transform to the white phase particles with irregular shape due to a high concentration of Cu [9]. The composition of phase A in sample 1 was close to that of the liquid phase of reaction 3. This fact indicated that these white phases mostly came from the liquid phase of reaction 3. However, in the DSC curve of the green compact, no evident endothermic peaks were detected at 507 and 548 °C, and only one endothermic peak at 525 °C was discernible. This may be due to the overlap of the endothermic peaks of reactions 3 and 4. A more detailed DSC experiment should be designed to verify this judgment.

Furthermore, the compositions of phase B in sample 1 fluctuated greatly in different locations (Table 2). This fact can be explained as follows. First, the holding time at 580 °C for sample 1 was very short, and the inter-diffusion between Al and Cu was not sufficient in the solid state (would be discussed later). Thus, some Cu particles did not transform to Al_2Cu completely in sample 1. The study about the sintering behavior of Al–10Pt–4.5Cu (wt%) mixed powders suggested that a small quantity of Al_4Cu_9 would form when the mixed powders were heated to below 550 °C, and Al_4Cu_9 would transform to Al_2Cu after the mixed powders was heated at 550 °C for 1 h [14]. Second, the reactive temperature of reaction 4 is close to 580 °C, so reaction 4 might proceed partly in sample 1 because of the short holding time. When the holding time extended to 15 min (sample 3), the composition of the white phases containing Al and Cu became stable and was close to the liquid phase of reaction 4. This indicted that all the Al_2Cu had transformed to the liquid phase due to an extended reactive time.

The liquid phase in the earlier stage of liquid phase sintering of elemental powders was transient [13, 15]. Once the liquid phase appeared, the alloying elements would be drawn from the liquid phase into the solid solution of aluminum. At last, all the liquid phase was absorbed into the Al particles if the content of the alloying elements was lower than their equilibrium solubility. In this study, the liquid phase containing Al, Cu, and Mg formed earlier than that containing Al and Cu, and the addition of Mg was only 1.8 wt%, which is much lower than the equilibrium solubility of Mg in Al at 580 °C, so after holding for 30 min, the liquid phase containing Al, Cu, and Mg disappeared. The Cu addition was 4.5 wt% in this study, which is higher than the equilibrium solubility of Cu in Al at 580 °C according to the Al–Cu phase diagram [12]. So after the compact was held at 580 °C for 30 min, the liquid phase containing Al and Cu still existed while its size decreased compared with that in samples 1 and 2. After the concentration of Cu in Al reached its equilibrium solubility at 580 °C (about 3.5%), part of the liquid phase remained and reached the state of dynamic equilibrium [15]. In such a state, the liquid phase would prefer to form at the boundaries of the Al particles and the grains (Fig. 3d) where the free energy was higher than the other locations. After quenching, the liquid phase transformed to fine white phase particles (Fig. 3d).

The increase of the white phase particles after HP was attributed to the following reasons (compared Fig. 6 with 3d). First, the compact was fundamentally densified after HP. The elimination of voids could decrease the diffusion distance of Cu and Mg and increase the diffusion paths. Second, the pressing caused the crack of oxide shell on the surface of the Al particles [16], thereby contributing to the diffusion of alloying elements [15, 17]. Third, the temperature of the compacts might be elevated during the pressing due to friction between compact and die, benefiting the diffusion of alloying elements. These three factors caused the increase of the amount of liquid phase and therefore more white phase particles remained after quenching.

Diffusion of elements during HP

Generally, the Al particle was covered by an oxide shell, which was a barrier to the diffusion of alloying elements. Tang et al. [17] investigated the effect of oxide shell on the diffusion of elements during aluminum sintering. The results suggested that the diffusion coefficient of Cu decreased from 1.4×10^{-13} to 6.7×10^{-17} m^2/s at 550 °C due to the existence of oxide shell. So in the earlier sintering stage, the concentration of Cu was lower and inhomogeneous in the Al particles due to the low diffusivity and the short diffusion time. As shown in Fig. 4, with the increase of holding time at 580 °C, the concentration of Cu increased and became more homogeneous in the Al particles. This can be attributed to the following reasons. First, the longer holding time was helpful for the diffusion and homogenization of Cu. Second, the liquid phase formed when the compact was held at 580 °C, the diffusion between liquid and solid was significantly faster than that between solid and solid [10]. After holding for 60 min, the concentration of Cu reached 3.4 wt%, which is close to the equilibrium solubility (about 3.5%) of Cu in Al at 580 °C according to the Al–Cu binary phase diagram [12]. This implies that the diffusion of Cu had completed, which was in good agreement with the fact that the white phases containing Al and Cu disappeared in sample 4 (Fig. 3d).

Mg is highly reactive and the free energy for its oxide formation is lower than that of Al, so the oxide shell on the Al particles would react with Mg to form some oxide of Mg at about 500 °C [13, 18]. In this case, the oxide shell of the Al particles would be broken partly. Furthermore, the liquid phase containing Mg appeared earlier than that containing Cu. So it is expected that the diffusion of Mg was easier than that of Cu. However, the concentration of Mg was still only about 0.9% when the compact was held at 580 °C for 60 min, which was only half of the Mg addition and was much lower than the equilibrium solubility of Mg in Al at 580 °C (about 5%).

The elemental maps of sample 4 (Fig. 5c) indicated that Mg was preferentially distributed at the boundaries of the initial Al particles and in the clusters of SiC particles. The aggregation of Mg near the interfaces of Al and SiC was observed by many researchers [19, 20]. Apart from the aggregation at the interface, Mg would concentrate near the surface region of the Al particles because of the existence of oxide shell. For example, Kimura et al. [18] found that for the air-atomized Al–Fe–Ni–Mg powder, Mg atoms would move to the surface of powders and concentrate on the surface region of the Al particles above 300 °C. The aggregation of Mg at the Al/SiC interface and on the oxide shell of the Al particles caused the lower concentration of Mg in the interior of the Al particles.

Microstructure evolution during cooling after HP

Eutectic formed when the compact was cooled from 580 °C to eutectic reaction temperature. As discussed in "Formation of liquid phases during HP", the composition of the liquid phase after a long time holding at 580 °C was close to that of Al–4.5Cu–1.8 Mg, so eutectic reactions 3 and 4 would occur during consolidation according to the Al–Cu–Mg ternary phase diagram [12]. In the XRD pattern of the matrix alloy (Fig. 10), the peaks of Al_2CuMg and Al_2Cu also confirmed this judgment. However, in the XRD pattern of sample 6, Mg_2Si peaks replaced Al_2CuMg peaks (Fig. 10). This was similar with the results of Kiourtsidiss et al. [21]. Their results showed that in SiCp/2024Al composite fabricated by squeeze casting technique, Al_2Cu and Mg_2Si were detected, while in 2024Al alloy fabricated by the same method Al_2CuMg and Al_2Cu were found. They reported that SiC particles reacted with molten Al during processing of composites at temperature above 710 °C:

$$4Al + 3SiC \rightarrow Al_4C_3 + 3Si. \quad (5)$$

As a result, the Al–Cu–Mg–Mn matrix actually altered to the Al–Cu–Mg–Si matrix. According to Mondolfo [12], in the Al–Cu–Mg–Si alloys, Mg_2Si was the first phase to precipitate. In this study, the HP temperature was only 580 °C, reaction 5 could not occur. However, the previous studies suggested that there were usually a small quantity of Si and SiO_2 on the surface of SiC [21, 22]. The chemical reaction during HP may take place as follows:

$$4Al + 3SiO_2 \rightarrow 2Al_2O_3 + 3Si \quad (6)$$

$$2Mg + SiO_2 \rightarrow 2Mg_2O + Si \quad (7)$$

$$Al_2O_3 + Mg_2O \rightarrow MgAl_2O_4. \quad (8)$$

Si would be entrapped into the liquid phase during HP, and Mg_2Si would precipitate first when the compact was cooled from 580 °C to room temperature. The formation of Mg_2Si reduced the concentration of Mg and then increased the Cu/Mg ratio in the liquid phase. The decreased Cu/Mg ratio did not facilitate the formation of Al_2CuMg, so there was no identifiable peak of Al_2CuMg in the XRD pattern of sample 6 (Fig. 10). And in the elemental maps of sample 6, some oxides of Mg would also verify that reactions 7 and 8 occurred during HP.

Rodrigo et al. [23] also found that there was Mg_2Si on the surface of the SiC particles in the extruded SiCp/2009Al composite prepared by pre-alloyed powders. The size of Mg_2Si was only about 200 nm [23]. By comparison, in this study, the Mg_2Si exhibited a size of larger than 2 μm (Fig. 8). This might be attributed to the following reasons. First, the composite in Ref. [23] was examined after extrusion. The Mg_2Si might be broken during extrusion.

Second, during the HP of PRAMC fabricated by elemental powders, some Mg particles and Mg-rich liquid phases would contact with the SiC particles directly before the diffusion reached the state of equilibrium, but for the PRAMC fabricated by pre-alloyed powders, the phase contacting with the SiC particles during HP or sintering was the pre-alloyed Al particles and the equilibrium liquid phase, in which the concentration of Mg was less than 6% according to the Al–Cu–Mg ternary phase diagram [12]. The higher concentration of Mg around the SiC would result in the formation of coarser Mg_2Si than that in Ref. [23].

Element distribution after solution treatment

After the solution treatment, Al_2Cu dissolved into the Al matrix, producing homogeneous distribution of Cu in the matrix. But Mg was still preferentially distributed in the boundaries of the Al particles and in the clusters of SiC particles (Fig. 9). As discussed in "Diffusion of elements during HP", Mg aggregated at the interface of Al and SiC and the oxide shell on the surface of the initial Al particles. The aggregation of Mg also indicated that the solution treatment could not achieve homogeneous distribution of Mg. The distribution of Mg could be modified by subsequent hot working such as extrusion and rolling which could not only improve the homogeneity of SiC distribution [24] but also break down the oxide shell of the Al particles [16]. In addition, there were still some un-dissolved Mg-rich compounds after the solution treatment. EDS analyses indicated that the composition of the Mg-rich compounds was similar to that in sample 6 before the solution treatment (Table 3). According to the previous study [25], the oxide of Mg such as $MgAl_2O_4$ and MgO could not dissolve into the Al matrix, while Mg_2Si dissolved into the matrix during the solution treatment. The XRD result of sample 6 after the solution treatment also indicated that most of Mg_2Si dissolved into the matrix (Fig. 10). But, there were still some un-dissolved silicides of Mg after the solution treatment according to the EPMA results (Fig. 9). This is attributed to relatively low solution treatment temperature adopted in this study. For Al–Cu–Mg alloys, the solution treatment temperature is usually at 495 ± 5 °C. However, some aluminum alloys or particle-reinforced Al matrix composites with Mg_2Si as the strengthening precipitates were usually solutionized at about 530 °C [7]. Several studies indicated that for PM 2xxx Al-based composites, higher solution treatment of 530–540 °C produced an optimum combination of strength and ductility [26–28]. So the solution treatment temperature for these composites fabricated using elemental powders needs future optimization.

Conclusions

1. There were two types of eutectic liquid phases with different compositions after the compact was heated to 580 °C. One located at the boundaries of the initial Al particles contained Al and Cu, and the other near the original site of the Mg particles contained Al, Cu, and Mg. After the compact was held at 580 °C for 60 min, the eutectic liquid phase was absorbed into the Al matrix and some equilibrium liquid formed at the boundaries of the initial Al particles.
2. After the compact was held at 580 °C for 60 min, Cu was homogeneously distributed in the matrix, but Mg was still preferentially distributed in the cluster of SiC and near the boundaries of the initial Al particles.
3. In the as-hot pressed composites Al_2Cu and Mg_2Si and some oxides of Mg were detected. After the solution treatment, Al_2Cu dissolved into the Al matrix, producing uniform distribution of Cu in the matrix, but some Mg-rich compounds (silicide and oxide of Mg) did not dissolved into the matrix completely and Mg was preferentially distributed near the boundaries of the Al particles and in the clusters of SiC.

References

1. Miracle DB (2005) Compos Sci Technol 65:2526
2. Rosso M (2006) J Mater Proc Technol 175:364
3. Lloyd DJ (1994) Int Mater Rev 39:1
4. Shang JK, Ritchie RO (1989) Acta Metall 37:2267
5. Davidson DL (1989) J Mater Sci 24:681. doi:10.1007/BF01107459
6. Srivatsan TS, Hajri MA, Smith C, Petraroli M (2003) Mater Sci Eng A 346:91
7. Appendino P, Badini C (1991) Mater Sci Eng A 135:275
8. Singh PM, Lewandowski JJ (1993) Metall Trans A 24:2531
9. Kim SC, Kim MT, Lee S, Chung H, Ahn JH (2005) J Mater Sci 40:441. doi:10.1007/s10853-005-6101-7
10. Zhou J, Duszczyk J (1999) J Mater Sci 34:545. doi:10.1023/A:1004594628862
11. Ogel B, Gurbuz R (2001) Mater Sci Eng A 301:213
12. Mondolfo LF (1976) Aluminium alloys: structure and properties. Butterworth & Co. Ltd., London
13. Schaffer GB, Sercombe TB, Lumley RN (2001) Mater Chem Phys 67:85
14. Zhu M, Ouyang LZ, Wu ZF, Zeng MQ, Li YY, Zou J (2006) Mater Sci Eng A 434:352
15. Liu ZY, Sercombe TB, Schaffer GB (2007) Metall Mater Trans A 38:1351
16. Song M, He YH (2010) Mater Des 31:985
17. Tang F, Anderson IE, Biner SB (2002) J Light Metals 2:201
18. Kimura A, Shibata M, Kondoh K, Takeda Y, Katayama M, Kanie T, Takada H (1997) Appl Phys Lett 70:3615
19. Strangwood M, Hippsley CA, Lewandowski JJ (1990) Scr Metall Mater 24:1483
20. Nutt SR, Carpenter RW (1985) Mate Sci Eng 75:169

21. Kiourtsidis GE, Skoliano SM, Litsardakis GA (2004) Mater Sci Eng A 382:351
22. Urena A, Martinez EE, Rodrigo P, Gil L (2004) Compos Sci Technol 64:1843
23. Rodrigo P, Poza P, Utrilla V, Urena A (2009) J Alloy Compd 479:451
24. Slipenyuk A, Kuprin V, Milman Y, Goncharuk V, Eckert J (2006) Acta Mater 54:157
25. Mcleod AD, Gabrye CM (1992) Metall Trans A 23:1279
26. Ma ZY, Lu YX, Luo M, Bi J (1995) J Mater Sci Technol 11:291
27. Thomas MP, King JE (1996) Compos Sci Technol 56:1141
28. Jin P, Xiao BL, Wang QZ, Ma ZY, Liu Y, Li S (2011) Mater Sci Eng A 528:1504